

First-principles study of hydrogen adsorption in metal-doped COF-10

Miao Miao Wu,^{1,2} Qian Wang,^{2,a)} Qiang Sun,^{1,2} Puru Jena,² and Yoshiyuki Kawazoe³

¹Department of Advanced Materials and Nanotechnology and Center for Applied Physics and Technology, Peking University, Beijing 100871, China

²Department of Physics, Virginia Commonwealth University, Richmond, Virginia 23284, USA

³Institute for Materials Research, Tohoku University, Sendai 980-8577, Japan

(Received 17 June 2010; accepted 28 September 2010; published online 21 October 2010)

Covalent organic frameworks (COFs), due to their low-density, high-porosity, and high-stability, have promising applications in gas storage. In this study we have explored the potential of COFs doped with Li and Ca metal atoms for storing hydrogen under ambient thermodynamic conditions. Using density functional theory we have performed detailed calculations of the sites Li and Ca atoms occupy in COF-10 and their interaction with hydrogen molecules. The binding energy of Li atom on COF-10 substrate is found to be about 1.0 eV and each Li atom can adsorb up to three H₂ molecules. However, at high concentration, Li atoms cluster and, consequently, their hydrogen storage capacity is reduced due to steric hindrance between H₂ molecules. On the other hand, due to charge transfer from Li to the substrate, O sites provide additional enhancement for hydrogen adsorption. With increasing concentration of doped metal atoms, the COF-10 substrate provides an additional platform for storing hydrogen. Similar conclusions are reached for Ca doped COF-10.
© 2010 American Institute of Physics. [doi:10.1063/1.3503654]

I. INTRODUCTION

Hydrogen, a clean and “renewable” energy carrier, is considered to play a critical role in a new, decentralized energy infrastructure that can provide power to vehicles, homes, and industries. However, one of the biggest challenges in a new hydrogen economy is finding hydrogen storage materials that must meet stringent requirements for mobile applications, namely, high gravimetric and volumetric density, fast kinetics, and favorable thermodynamics. No materials are available that meet all these requirements simultaneously. In light materials hydrogen is either bound weakly or strongly. In order to have desired kinetics for release, hydrogen stored in quasimolecular form is highly desirable, since the interaction of hydrogen molecule with the substrate is intermediate between van der Waals and chemical interaction. Since there is not enough space in conventional bulk materials to accommodate H₂ molecules, high surface area materials like porous materials are hotly pursued. These include metal organic frameworks (MOFs) and covalent organic frameworks (COFs). Due to the large mass of metal atoms such as Cu and Zn in MOFs, the gravimetric density for hydrogen storage is quite low. This shortcoming can be avoided in COFs, where the materials are composed of light elements (e.g., C, B, and O) linked by strong covalent bonds. However, the problem is that H₂ molecules are only weakly adsorbed on COFs. Pathways to enhance the adsorption while keeping high gravimetric density have become a key issue in materials design for hydrogen storage.

One of the strategies is to dope COFs with light metal atoms. Among these lithium is of special interest, since it is the lightest metal in the periodic table and unlike transition

metal atoms it does not cluster on carbon fullerenes and nanotubes. In addition, an isolated positive Li ion can adsorb up to six H₂ molecules with adsorption energy that lies between van der Waals and chemical bonding.¹⁻³ When Li atoms are deposited on C₆₀ fullerene, charge transfer makes Li atoms positively charged which then bind hydrogen quasimolecularly.⁴ The binding of hydrogen to Li can be further improved by doping C₆₀ with B.⁵ These findings have motivated researchers to extend the idea of metal doping to MOFs.⁶⁻¹¹ It has been found that clustering of transition metal atoms like Sc and Ti on a substrate is one of the key factors affecting the storage performance,¹² since metal clustering would reduce greatly the amount of stored hydrogen.

COFs belong to a class of porous polymeric materials with covalent bonds between C–C, C–O, and B–O. They usually have rigid structure, low densities, and exhibit exceptional thermal stabilities (to temperatures up to 600 °C). Their specific surface areas surpass those of well-known zeolites and porous silicates.¹³ Recently, a member of the COF family, COF-10, which is a two-dimensional (2D) mesoporous material, has been synthesized¹⁴ through cocondensation reactions between 2,3,6,7,10,11-hexahydroxy triphenylene (HHTP) and 4,4'-biphenyldiboric acid (BPDA). Under appropriate low-pressure regions of the isotherms, it has a surface area of 2080 m² g⁻¹, pore volume of 1.44 cm³ g⁻¹, and one dimensional pore diameter of 34 Å. Furukawa and Yaghi carried out an extensive experimental study of storage of hydrogen, methane, and carbon dioxide in the COF materials and found that three-dimensional (3D) COFs (such as COF-102 and COF-103) outperform 2D COFs (COF-1, COF-5, COF-6, COF-8, and COF-10) in their uptake capacities for hydrogen.¹⁵ More recently, they found that COF-10 shows an exceptional capacity for ammonia.¹⁶ The simulation of H₂ uptake behavior in COF-1 (Ref. 17)

^{a)}Electronic mail: qwang@vcu.edu.

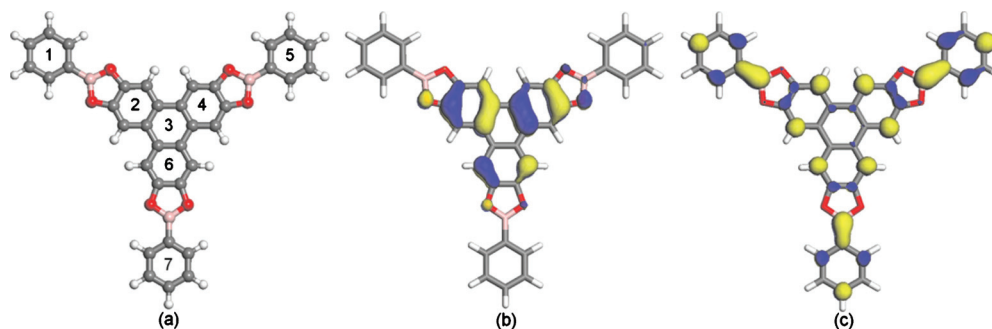


FIG. 1. (a) Geometry, (b) HOMO, and (c) LUMO of TBE molecule. The sites 1, 2, ... indicate where metal atoms are introduced to study their preferred structure.

and 3D COFs, including COF-102, CoF-103, COF-105, and COF-108, has been performed by several groups.^{18–21} It has been predicted that some COFs can store greater amounts of H₂ than MOFs and Li or Mg doping can enhance hydrogen adsorption. More interesting, Cao *et al.*¹⁹ predicted that Li-doped 3D COFs are the most promising candidates for hydrogen storage to date based on first-principles calculations. However, the theoretical study on pure or metal-decorated COF-10 for hydrogen storage is still lacking. One wonders if this 2D COF material has the potential for hydrogen storage through Li doping and if clustering of the metal atoms is also energetically unfavorable, as is the case in carbon fullerenes^{4,22} and nanotubes.²³

In this paper, we focused on studying the effect of Li doping in COF-10 on hydrogen adsorption to search for high capacity COF-based hydrogen storage materials. To this end, some key questions need to be addressed. For example, what sites Li atoms like to occupy? Do they prefer to cluster? Does the metal doping affect the structure and electronic properties of the substrate itself? The answers to these questions are important to better understand and design COFs for hydrogen storage. We note that Ca also has the capability of enhancing hydrogen adsorption^{24–27} and has a weak tendency of clustering.²⁸ Therefore, we have also explored the effect of Ca doping on the hydrogen storage properties of COF-10.

II. COMPUTATIONAL PROCEDURE

The calculations were carried out by using density functional theory (DFT) and generalized gradient approximation (GGA) for exchange-correlation energy. We used the Perdew–Wang 91 form²⁹ for GGA and a plane-wave basis set within the projector-augmented-wave (PAW) method originally developed by Blöchl³⁰ and adapted by Kresse and Joubert³¹ in the *Vienna ab initio simulation package*. The particular advantage of the PAW method over the ultrasoft pseudopotentials is that the pseudization of the augmentation charge can be avoided. Though many methods are available for this study, previous benchmark calculations^{32,33} showed that the results using PW91 functional are close to those obtained from MP2 level of theory for describing the noncovalent intermolecular interactions. Some studies^{34–36} have also demonstrated that PW91 is reliable for evaluating the hydrogen adsorption. The structure optimization was symmetry unrestricted and was carried out using conjugate-gradient algorithm. The convergence for the energy and the

force were set to 0.0005 and 0.01 eV/Å, respectively. The energy cutoff was set to 400 eV based on our previous study.¹² We used a supercell approach where the clusters under investigation were surrounded by 15 Å of vacuum space along the *x*, *y*, and *z* directions. Due to the large supercell, the Γ point was used to represent the Brillouin zone.

To reduce the computational demand, we have used a fragment of the COF-10, triboronate ester (C₃₆H₂₁B₃O₆), as shown in Fig. 1. This is labeled as TBE, which is a repeat unit saturated with a hydrogen atom on each end. The structure consists of one HHTP molecule and three five-membered boronate ester rings (C₂O₂B) connecting three benzene rings. This can be viewed as half of the BPDA molecule with *D*_{3h} symmetry. The optimized geometry is shown in Fig. 1(a), where we numbered the seven benzene rings for the following discussions. The highest occupied molecular orbital (HOMO) is mainly contributed by the central part in TBE [Fig. 1(b)], while the lowest unoccupied molecular orbital (LUMO) is almost homogeneously distributed over the whole TBE [Fig. 1(c)].

III. RESULTS AND DISCUSSION

We began with one Li atom doped in TBE. To determine the preferred site of Li, we have chosen five nonequivalent sites for Li to occupy, thus generating five configurations of Li-TBE. Configurations *I*₁, *I*₂, and *I*₃ correspond to introducing Li atom on top of the hollow site of no. 1 benzene ring, B–C bridge site and B on top site next to the ring in Fig. 1(a), respectively. In configurations *I*₄, Li atom is introduced at top of the hollow site of the five-membered ring of B–O–C–C–O between nos. 1 and 2 benzene rings. In configurations *I*₅, the Li atom is on the top of the hollow site of no. 2 benzene ring. Optimizations show that the first three initial configurations lead to a stable state, as shown in Fig. 2(a)(1), where the Li atom is on the top hollow site of no. 1 benzene ring. We name it as site-1 which has a binding energy of 1.05 eV. Li–C bond length is found to be 2.20 Å. The latter two initial configurations lead to the metastable state. We name the site where Li atom is on the top hollow site of no. 2 benzene ring as site-2. This site lies 0.2 eV higher in energy than site-1. It is interesting to note that Li doping has little effect on the HOMO [Fig. 2(b)(1)], but it changes the LUMO substantially [Fig. 2(c)(1)]. The LUMO is highly inhomogeneous and is concentrated on the ring having Li. The HOMO-LUMO gap is calculated to be 0.43 eV.

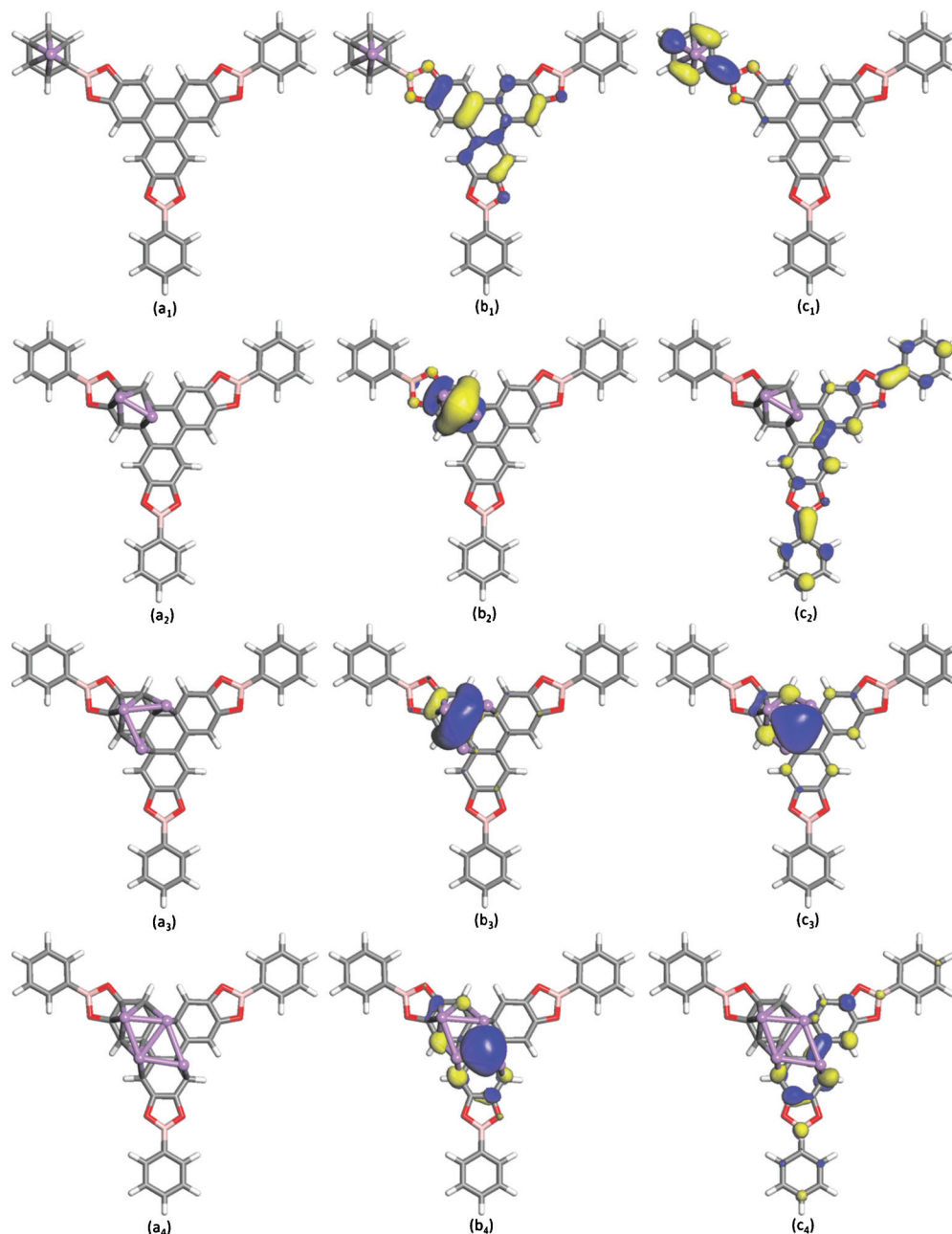


FIG. 2. (a) Geometry, (b) HOMO, and (c) LUMO orbitals for Li-TBE, 2Li-TBE, 3Li-TBE, and 4Li-TBE, respectively. The isosurface value is 0.04 a.u.

We next introduced two lithium atoms to the TBE. There are again many possible sites for two Li atoms to occupy. We have considered six different initial configurations and only introduced Li atoms on the top hollow sites of the benzene rings based on our finding as discussed above. The six configurations are labeled as (1,2), (1,3), (1,5), (1, $\bar{2}$), (2,3), and (2, $\bar{3}$). Here the numbers stand for the benzene rings as shown in Fig. 1(a) and the negative sign denotes Li atoms occupying the opposite side of the ring. For example, site (1,2) indicates that Li atoms occupy the hollow sites above the rings marked 1 and 2 in Fig. 1, while site (1, $\bar{2}$) indicates that one Li atom is above benzene ring 1 while the other is below benzene ring 2. We found that the lowest energy configuration is (2,3). Here the two Li atoms form a dimer with the Li–Li bond length of 2.43 Å. They reside on the top of

no. 2 benzene ring, as shown in Fig. 2(a)(2). The binding energy for each Li atom is 1.11 eV and the average Li–C bond length is 2.18 Å. In Table I we give the relative energy for all the configurations considered. The Li dimer caused a local distortion in geometry and the structure was bent outward. The HOMO is mainly on Li dimer [Fig. 2(b)(2)], while the LUMO is on other rings [Fig. 2(c)(2)].

To find the preferred configuration when three Li atoms are introduced, we considered five configurations labeled (1,2,3), (1,3,5), (1,5,7), (2,3,4), and (2,4,6). The configuration of (2,4,6) gave the lowest energy, approximately 0.21 ~ 0.44 eV lower in energy than the others (Table I). In the lowest energy configuration, the three Li atoms move together forming an isosceles triangle with Li–Li bond lengths of 2.77, 2.77, and 3.21 Å, as shown in Fig. 2(a)(3). This

TABLE I. The relative energy (ΔE) (in eV) and the binding energy per Li atom (BE/Li) (in eV) for doping two, three, and four Li atoms at different sites on TBE. The numbering of sites for initial configurations (Config.) is explained in the text. For example, (1,2) configuration indicates that two Li atoms were introduced at sites 1 and 2 in Fig. 1.

Config.	1Li-TBE		Config.	2Li-TBE		Config.	3Li-TBE		Config.	4Li-TBE	
	ΔE	BE/Li		ΔE	BE/Li		ΔE	BE/Li		ΔE	BE/Li
(Site-1)	0.00	1.05	(1,2)	0.05	1.09	(1,2,3)	0.38	1.02	(1,3,5,7)	0.66	1.06
(Site-2)	0.20	0.85	(1,3)	0.30	0.96	(1,3,5)	0.21	1.08	(1, $\bar{3}$,5,7)	0.64	1.07
			(1,5)	0.15	1.04	(1,5,7)	0.32	1.04	(2,3,4,6)	0.65	1.06
			(1, $\bar{2}$)	0.29	0.97	(2,3,4)	0.44	1.00	(2, $\bar{3}$,4,6)	0.51	1.10
			(2,3)	0.00	1.11	(2,4,6)	0.00	1.15	(Rhomb)	0.00	1.23
			(2, $\bar{3}$)	0.26	0.98			(Tetrahedron)	0.04	1.22	

geometry can be considered as adding one more Li atom to the 2Li-TBE structure, but unlike the 2Li-TBE, the introduction of three Li atoms does not cause much distortion in geometry. And in this case, the HOMO and LUMO are on the Li₃ cluster [see Fig. 2(b)(3) and Fig. 2(c)(3)].

To find the equilibrium structure of four Li atoms, we studied six initial configurations. The first four are labeled (1,3,5,7), (1, $\bar{3}$,5,7), (2,3,4,6), and (2, $\bar{3}$,4,6). The fifth and the sixth configurations are based on the 3Li-TBE by adding one more Li either forming a rhombus or a tetrahedron, respectively. The structure optimizations indicate that the rhombus configuration has the lowest energy while the tetrahedron is only 0.04 eV higher in energy. The remaining four configurations are much higher in energy with the energy difference lying in the range of 0.51–0.66 eV. The HOMO is mainly on Li atoms, while the LUMO is mainly on C sites next to the Li₄ cluster. This is different from other cases we discussed above. It is clear that Li atoms prefer to cluster, which has been further confirmed by adding more Li atom to the TBE. For instance, the clustering configuration of seven Li on the TBE with compact C_{3v} structure is found to be 0.78 eV lower in energy than the one with one Li on each top hollow site of the seven numbered benzene rings in Fig. 1(a).

Next we discuss hydrogen adsorption. One of the quantities we used to measure the thermodynamics is adsorption energy (AE), which is defined as the energy difference between the complex and its fragments,

$$AE(H_2) = - [E(TBE + mLi + nH_2) - E(TBE + mLi) - E(nH_2)]/n.$$

Here m is the number of Li atoms and n is the number of hydrogen molecules. For Li-TBE, when one H₂ molecule is introduced to Li site, the equilibrium distance H₂ and Li site is 2.13 Å, and the bond length of H₂ is elongated to 0.76 Å. The adsorption energy is found to be 0.12 eV. When two and three H₂ molecules are trapped, the distance to Li changes to 2.18 and 2.23 Å, and the adsorption energy is slightly reduced to 0.11 eV. In 4Li-TBE, four Li atoms form a rhombus, with each Li site trapping one H₂ molecule [Fig. 3(a)]; the average adsorption energy is 0.14 eV/H₂. When two H₂ molecules are initially introduced to each Li site, the structure optimization shows that only six of them can be trapped due to the steric hindrance [Fig. 3(b)]. The average adsorption energy is found to be 0.15 eV/H₂, which is larger than

that for 4Li-TBE-4H₂. The distance to Li also increases to 2.33 Å (Table II). These changes cannot be understood based just on the polarizing interactions of Li ions. In fact in this case, some H₂ molecules are closer to the charged O sites and the added interaction with O sites increases the adsorption energy. Thus, we see that metal doping, due to charge transfer to the substrate, cannot only make it become the trap site but also additional adsorption induced on the substrate itself can enhance adsorption energy. Therefore, as the doping concentration increases the geometry and the interactions become complicated. There are two competing factors associated with high doping concentration; clustering of Li atoms reduces the available Li site for hydrogen adsorption while additional adsorption induced by the substrate can bind hy-

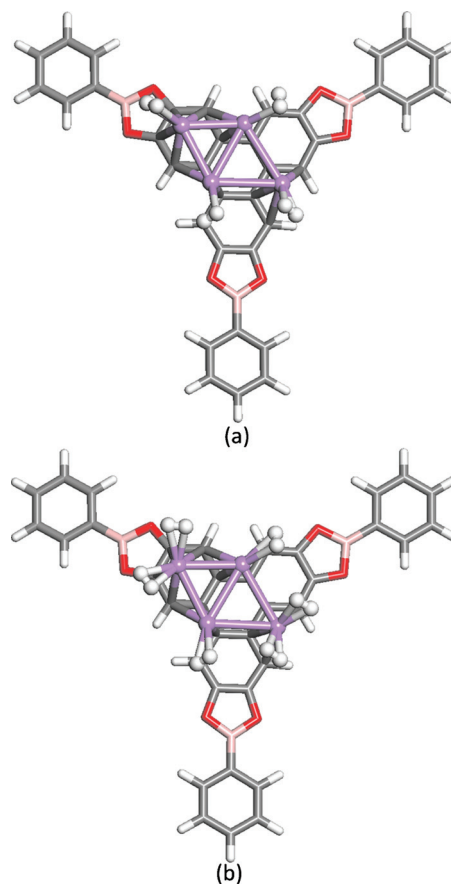


FIG. 3. Optimized geometry of (a) 4Li-TBE-4H₂ and (b) 4Li-TBE-6H₂.

TABLE II. The adsorption energy per H_2 (AE/H_2) (in eV), the average bond lengths for C–Li, Li–H, and H–H bonds (in angstrom), and the energy gaps (in eV) of TBE doped with one Li and four Li atoms, respectively.

Clusters	AE/H_2	C–Li	Li–H	H–H	Gap
Li-TBE+1 H_2	0.12	2.21	2.13	0.76	0.37
Li-TBE+2 H_2	0.11	2.23	2.18	0.76	0.39
Li-TBE+3 H_2	0.11	2.26	2.23	0.76	0.46
4Li-TBE+4 H_2	0.13	2.22	1.98	0.76	0.64
4Li-TBE+6 H_2	0.15	2.33	1.97	0.77	0.76

drogen on the substrate. In our calculations we have not included zero-point energies (ZPEs) or thermal corrections. Previous studies have found that the ZPE of H_2 in porous materials lies in the range of 0.01–0.02 eV/ H_2 .^{37–39} Based on these results, we feel that ZPE corrections will not have significant effect on our calculated adsorption energy. Thermal energy corrections at room temperature are of the order of meV and the adsorption energy would lie in the range of 0.08–0.12 eV, which is close to the energy window of 0.1–0.2 eV/ H_2 required for applications under ambient thermodynamic conditions.⁴⁰

We note that the Li-doped 2D COF-10 is unlike the 3D COFs^{18,19} due to their spatial structures and chemical constitutions. Although the average binding energies per Li in both systems are comparable (namely, 1.05, 1.11, 1.15, and 1.23 eV/Li for one to four Li atoms on the TBE of COF-10 versus 1.08 eV/Li for eight Li atoms on the TBPM of 3D COFs),¹⁹ the hydrogen adsorption energy of the Li-doped COF-10 is smaller than that of the Li-doped 3D COFs. For instance, the adsorption energy of the Li ion-doped 3D COFs was found to be 0.28 eV/ H_2 ,¹⁸ while that for the Li-doped COF-10 is in the range of 0.11–0.15 eV. We recall from the case of $Li_{12}C_{60}$ (Ref. 4) that due to the special geometry of the fullerene, 12 Li atoms are separately capped on 12 pentagons of C_{60} and each Li site has enough space to trap hydrogen molecules. However, Li atoms on COF-10 tend to cluster. We also recall that C_{60} uniformly coated with a layer of Ca has been shown to be an effective trap of hydrogen.²³ Therefore, we explored the possibility of Ca doping to enhance the capacity of hydrogen storage in COF-10.

Following similar procedure described above, we have further studied Ca doping. We found that Ca atoms also have the tendency to cluster in COF-10. For this study we introduced four Ca onto the TBE substrate. Four different initial configurations with Ca atoms occupying (1,3,5,7) and

(1, $\bar{3}$,5,7) sites in Fig. 1 and forming both planar rhombus and tetrahedral geometries were considered. Analogous to the case of 4Li-TBE structure, the lowest energy configuration in the Ca doped case is the one where four Ca atoms form a rhombus cluster. This is about 0.80 eV lower in energy than that of (1,3,5,7) site. The relaxed structure and the HOMO and LUMO orbitals for the lowest energy configuration are plotted in Fig. 4. They show that most of the frontier orbitals for both the HOMO and LUMO are mainly focused on Ca atoms, while the LUMO of 4Li-TBE is mainly located on C sites near to the Li_4 cluster. Compared with Li, more charge is transferred to the substrate due to the higher valency of Ca. Therefore, Ca atoms carry larger positive charge than Li. This results in a stronger local electric field, larger polarization of the H_2 molecules, and higher binding energy of H_2 . The adsorption energy is 0.21 and 0.16 eV/ H_2 for Ca-TBE- H_2 and 4Ca-TBE-4 H_2 respectively. Therefore, Ca doping provides a better platform for enhancing hydrogen adsorption thermodynamics in COF-10.

IV. CONCLUSIONS

In summary, we have studied the potential of metal-doped COF-10 as hydrogen storage materials. We doped COF-10 with up to four Li and Ca atoms. We then studied the interaction of these doped metal atoms with up to three hydrogen molecules. Charge transfer from the metal atoms to COF-10 leaves the metal atoms in a positively charged state and hydrogen atoms are bound to these sites in quasimolecular form through the polarization mechanism.¹ However, unlike in the case of Li and Ca doped C_{60} , these metal atoms were found to cluster on the COF-10 substrate, the clustering of metal atoms in COF-10 not only slightly distorts the substrate outwardly but also reduces the available sites for hydrogen to be adsorbed. On the other hand, the charge induced

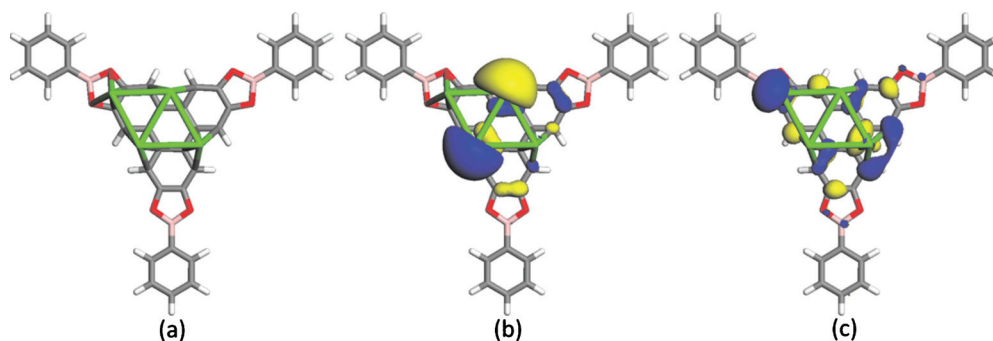


FIG. 4. (a) Geometry, (b) HOMO, and (c) LUMO orbitals for 4Ca-TBE.

on the COF-10 substrate helps to increase the adsorption energy. The frontier orbitals of COF-10 can be tuned by changing the doping concentration. As concentration of metal atoms increases, the COF-10 substrate becomes a more effective trap of hydrogen. These two competing factors show that metal-doped COF-10 could be a potential candidate for hydrogen adsorption.

ACKNOWLEDGMENTS

This work is partially supported by grants from the U.S. Department of Energy, the National Natural Science Foundation of China (NSFC-20973010, NSFC-10874007), and the China Scholarship Council. The authors thank the crew of the Center for Computational Materials Science, the Institute for Materials Research, Tohoku University (Japan), for their continuous support of the HITACH SR11000 supercomputing facility.

- ¹J. Niu, B. K. Rao, and P. Jena, *Phys. Rev. Lett.* **68**, 2277 (1992).
- ²B. K. Rao and P. Jena, *Europhys. Lett.* **20**, 307 (1992).
- ³J. Niu, J. B. K. Rao, P. Jena, and M. Manninen, *Phys. Rev. B* **51**, 4475 (1995).
- ⁴Q. Sun, P. Jena, Q. Wang, and M. Marquez, *J. Am. Chem. Soc.* **128**, 9741 (2006).
- ⁵Q. Sun, Q. Wang, and P. Jena, *Appl. Phys. Lett.* **94**, 013111 (2009).
- ⁶S. Yang, X. Lin, A. J. Blake, G. S. Walker, P. Hubberstey, N. R. Champness, and M. Schroder, *Nat. Chem.* **1**, 487 (2009).
- ⁷G. de Combarieu, S. Hamelet, F. Millange, M. Morcrette, M. Tarascon, G. Ferey, and R. Walton, *Electrochem. Commun.* **11**, 1881 (2009).
- ⁸D. Banerjee, S. J. Kim, and J. B. Parise, *Cryst. Growth Des.* **9**, 2500 (2009).
- ⁹T. Wu, J. Zhang, X. Bu, and P. Feng, *Chem. Mater.* **21**, 3830 (2009).
- ¹⁰E. Klontzas, A. Mavrandonakis, E. Tylianakis, and G. E. Froudakis, *Nano Lett.* **8**, 1572 (2008).
- ¹¹A. Mavrandonakis, E. Tylianakis, A. K. Stubos, and G. E. Froudakis, *J. Phys. Chem. C* **112**, 7290 (2008).
- ¹²Q. Sun, Q. Wang, P. Jena, and Y. Kawazoe, *J. Am. Chem. Soc.* **127**, 14582 (2005).
- ¹³A. P. Côté, A. I. Benin, N. W. Ockwig, M. O'Keefe, A. J. Matzger, and O. M. Yaghi, *Science* **310**, 1166 (2005).
- ¹⁴A. P. Côté, H. M. El-Kaderi, H. Furukawa, J. R. Hunt, and O. M. Yaghi, *J. Am. Chem. Soc.* **129**, 12914 (2007).
- ¹⁵H. Furukawa and O. M. Yaghi, *J. Am. Chem. Soc.* **131**, 8875 (2009).
- ¹⁶C. J. Doonan, D. J. Tranchemontagne, T. G. Glover, J. R. Hunt, and O. M. Yaghi, *Nat. Chem.* **2**, 235 (2010).
- ¹⁷P. Srepusharawoot, R. H. Scheicher, C. M. Araújo, A. Blomqvist, U. Pinsook, and R. Ahuja, *J. Phys. Chem. C* **113**, 8498 (2009).
- ¹⁸Y. Choi, J. Lee, J. Choi, and J. Kang, *Appl. Phys. Lett.* **92**, 173102 (2008).
- ¹⁹D. Cao, J. Lan, W. Wang, and B. Smit, *Angew. Chem., Int. Ed.* **48**, 4730 (2009).
- ²⁰E. Klontzas, E. Tylianakis, and G. Froudakis, *J. Phys. Chem. C* **113**, 21253 (2009).
- ²¹J. Lan, D. Cao, and W. Wang, *J. Phys. Chem. C* **114**, 3108 (2010).
- ²²F. Rabilloud, *J. Phys. Chem. A* **114**, 7241 (2010).
- ²³I. Cabria, M. J. López, and J. A. Alonso, *J. Chem. Phys.* **123**, 204721 (2005).
- ²⁴Q. Wang, Q. Sun, P. Jena, and Y. Kawazoe, *J. Chem. Theory Comput.* **5**, 374 (2009).
- ²⁵C. Ataca, E. Akturk, and S. Ciraci, *Phys. Rev. B* **79**, 041406 (2009).
- ²⁶X. Yang, R. Q. Zhang, and J. Ni, *Phys. Rev. B* **79**, 075431 (2009).
- ²⁷Y. Y. Sun, K. Lee, Y. H. Kim, and S. B. Zhang, *Appl. Phys. Lett.* **95**, 033109 (2009).
- ²⁸J. W. Mirick, C. H. Chien, and E. Blaisten-Barojas, *Phys. Rev. A* **63**, 023202 (2001).
- ²⁹Y. Wang and J. P. Perdew, *Phys. Rev. B* **44**, 13298 (1991).
- ³⁰P. E. Blöchl, *Phys. Rev. B* **50**, 17953 (1994).
- ³¹G. Kresse and J. Joubert, *Phys. Rev. B* **59**, 1758 (1999).
- ³²C. Enkvist, Y. Zhang, and W. Yang, *Int. J. Quantum Chem.* **79**, 325 (2000).
- ³³S. Tsuzuki and H. P. Lüthi, *J. Chem. Phys.* **114**, 3949 (2001).
- ³⁴Y. Y. Sun, K. Lee, L. Wang, Y. H. Kim, W. Chen, Z. Chen, and S. B. Zhang, *Phys. Rev. B* **82**, 073401 (2010).
- ³⁵F. Li, J. Zhao, B. Johansson, and L. Sun, *Int. J. Hydrogen Energy* **35**, 266 (2010).
- ³⁶Z. Zhou, J. Zhao, Z. Chen, X. Gao, T. Yan, B. Wen, and P. Schleyer, *J. Phys. Chem. B* **110**, 13363 (2006).
- ³⁷S. A. FitzGerald, J. Hopkins, B. Burkholder, and M. Friedman, *Phys. Rev. B* **81**, 104305 (2010).
- ³⁸L. Kong, G. Román-Pérez, J. M. Soler, and D. C. Langreth, *Phys. Rev. Lett.* **103**, 096103 (2009).
- ³⁹K. Sillar, A. Hofmann, and J. Sauer, *J. Am. Chem. Soc.* **131**, 4143 (2009).
- ⁴⁰S. K. Bhatia and A. L. Myers, *Langmuir* **22**, 1688 (2006).